Research Article Vol. 13, No. 3 / 1 Mar 2023 / Optical Materials Express 833

Optical Materials EXPRESS

3-W output power from a 2-μm InGaSb VECSEL using a hybrid metal-semiconductor Bragg reflector

NICOLAS HUWYLER,* MARCO GAULKE, JONAS HEIDRICH, MATTHIAS GOLLING, AJANTA BARH, AND URSULA KELLER

Ultrafast Laser Physics, Institute for Quantum Electronics, ETH Zürich, Auguste-Picard Hof 3, Zürich, 8092, Switzerland

*nhuwyler@phys.ethz.ch

Abstract: We present improved thermal management of an optically-pumped vertical external cavity surface emitting laser (VECSEL) at a center wavelength of around 2 μm. This was achieved with a backside-cooled, InGaSb-based VECSEL using a hybrid metal-semiconductor Bragg reflector. We demonstrate the fabrication of such a hybrid metal-semiconductor mirror by combining a copper mirror with 10.5 $AlAs_{0.08}Sb_{0.92}$/GaSb distributed Bragg reflector (DBR) pairs. Together with a thin 20 nm SiO_2 diffusion barrier we reach >99.9 % reflectivity at 2 μm. This allows for a thinner gain chip design compared to the standard DBR requiring 19.5 layer pairs. The structure thickness was reduced from 7.5 μm to 4.7 μm lowering the thermal resistance of the device from (2.79±0.16) K W^{-1} to (2.12±0.19) K W^{-1}. We demonstrate record high average continuous wave (cw) output powers of 3 W for backside-cooled InGaSb-based VECSELs.

1. Introduction

Optically-pumped vertical external cavity surface emitting lasers (VECSELs) [1] combine the wavelength flexibility of semiconductor bandgap engineering with excellent beam quality and simple cavity designs as well as high average output power. The VECSEL consists of a semiconductor gain reflector chip and an output coupler in a standing-wave linear cavity allowing for high average output power in a fundamental transverse mode. Passive modelocking can be obtained using an intracavity semiconductor saturable absorber mirror (SESAM) with a pulse repetition rate in the 1-100 GHz regime [2,3] set by the round trip group delay in the laser cavity. In addition, single-cavity dual-comb modelocking can be obtained with polarization [4] or spatial multiplexing [5]. A pulse repetition rate of 1 GHz requires a cavity length of 15 cm and is ideally suited for dual-comb applications [6] as demonstrated with molecular spectroscopy [7,8], THz spectroscopy [9] and picosecond ultrasonics [10,11] using single-cavity dual-comb lasers in the near-infrared regime without any further active stabilization.

Therefore there is a strong commercial interest to advance this laser technology towards the short-wavelength infrared (SWIR) and mid-infrared (MIR) regime for all such applications (see also review article [12]). Moving from the near-infrared to the SWIR wavelength regime the VECSEL technology has been expanded from the GaAs to the GaSb material platform, where InGaSb-based VECSELs have shown both high average power for cw [13,14] and cw modelocked operation [15].

We demonstrate in this paper that the thermal management of such longer wavelength VECSELs can be improved with a smaller thickness of the gain chip using a hybrid metal-semiconductor mirror. This approach does not require an expensive optical-quality intracavity heat spreader, improves the heat removal from the active layers for backside-cooled VECSEL chips and is also ideally suited for passive modelocking.

#485694 https://doi.org/10.1364/OME.485694
Journal © 2023 Received 13 Jan 2023; revised 19 Feb 2023; accepted 20 Feb 2023; published 1 Mar 2023

Optical Materials EXPRESS

1.1. Thermal management in VECSEL

Efficient heat removal from the VECSEL gain chip has a big impact on the performance. The fundamental pump-induced heating of the device results from the portion of the pump energy that is not converted to lasing photons. A significant part is transferred to phonons because of unavoidable carrier thermalization from the mismatch in pumping and lasing photon energies, referred to as the quantum defect in laser physics. Additionally, carrier leakage and non-radiative defect recombination lead to further energy losses and reduced pump efficiency. With increasing heat in the VECSEL gain structure, the emission wavelength redshifts and the standing laser field inside the gain chip becomes mismatched with the resonant periodic gain arrangement [16] of the InGaSb quantum wells (QWs) placed in the antinodes. Consequently, the VECSEL experiences a thermal rollover in output power for increasing pump powers. Thus, efficient heat removal from the active region combined with a small quantum defect and non-radiative defect recombination becomes the main strategy to achieve high-power operation [17].

The two main heat removal methods consist of a highly conductive heat spreader between the semiconductor gain mirror and the heat-sink, removing the heat either from the front or the back side of the chip. Front-side cooling requires a high optical-quality transparent heat spreader because it is placed inside a high-Q laser cavity. In contrast to edge-emitting semiconductor diode lasers, the gain of the VECSEL is much smaller with the optical cavity mode placed perpendicular to the gain QWs. Typically silicon carbide (SiC) or diamond is used on top of the gain mirror. Optical quality diamond is by far the best material for front-side cooling due to its intrinsic high thermal conductance of up to $2190\,\mathrm{W\,m^{-1}\,K^{-1}}$ [18] and wide transmission window. Transparent silicon carbide offers a cheaper and easier machinable alternative, however, at the expense of a lower thermal conductance of $325\,\mathrm{W\,m^{-1}\,K^{-1}}$ for 6H SiC [19].

Backside cooling is simpler for passive modelocking and does not require any optical-quality heat spreaders. Diamond is again the best choice, but metal heat spreaders, for example, made from copper, offer a cheap alternative with a thermal conductivity of $386\,\mathrm{W\,m^{-1}\,K^{-1}}$ [20]. Backside cooling is less efficient since the heat is removed through the highly reflective semiconductor distributed Bragg reflector (DBR). The thermal conductivity of the two main materials used in the DBR, which constitutes 80 % of the structure thickness, is 14 and $20\,\mathrm{W\,m^{-1}\,K^{-1}}$ for $AlAs_{0.08}Sb_{0.92}$ and GaSb, respectively [17]. Therefore, the thickness of the DBR plays a significant role in heat removal. Additionally, for the InGaSb VECSEL chip, the GaSb layers of the DBR are absorbing for pump wavelengths below 1720 nm, causing additional heating of the structure.

The backside-cooled device is grown in reverse order requiring substrate removal and processing but opening up the possibility to combine the semiconductor DBR with a metal mirror. A thinner DBR in combination with a metal mirror layer can then reach the desired >99.9% reflectivity of the gain mirror with as low as 7.5 mirror pairs for a gold mirror in comparison to the 19.5 mirror pairs for a full semiconductor based DBR. Therefore, the overall device thickness is significantly reduced at longer wavelengths. We use the thermal resistance to quantify the thermal properties of VECSEL chips and the efficiency of the heat transport through the structure. The thermal resistance scales with the structure thickness and is highly dependent on the thermal conductivity of the materials. Thus, we expect for a thinner structure both a reduction in thermal resistance and improved laser performance.

Hybrid metal-semiconductor mirrors have already been demonstrated for GaAs and InP-based VECSELs [21–25] and are summarized in Table 1. A variety of approaches were used to realize hybrid mirrors. Growing a full structure with consequently thinning the DBR with wet etching [22] or growing a design with fewer DBR pairs [21], the structures are completed with a 100-nm Al_2O_3 adhesion layer and an aluminium mirror. A lithographic patterning approach removes the need for the dielectric adhesion layer and allows for a more highly reflective gold mirror instead of aluminium, but with the trade-off of a significantly reduced gain chip surface and more critical alignment [23]. Direct metal deposition on the DBR using a 5-nm thick titanium layer

Optical Materials EXPRESS

as an adhesion for a gold mirror on GaAs and GaSb [24] or gold without titanium on InP [25] was also demonstrated. Even though the thermal resistance of these hybrid mirrors improved compared to the full semiconductor DBR, however, there were no significant improvements for the laser performance because the overall DBR thickness was not really a limitation in the near-infrared regime [22]. In contrast for the GaSb-based VECSELs, the impact of thinner semiconductor DBRs is expected to be larger due to both the low thermal conductivities of the $AlAs_{0.08}Sb_{0.92}$/GaSb materials and the thicker DBR layer pairs required for the longer lasing wavelength [17].

Table 1. Summary of previously demonstrated VECSELs using hybrid metal-semiconductor mirrors.

Material System	#Layer pairs	Adhesion layer	Metal	Fabrication technology	ref.
GaAs	11.5, 18.5, 28.5	100 nm Al_2O_3	Al	wet etching mirror	[21]
GaAs	11.5	90 nm Al_2O_3	Al	direct deposition	[22]
GaAs	14	100 nm Ti	Au	patterned mirror	[23]
GaAs, GaSb	27.5, 14.5	5 nm Ti	Au	direct deposition	[24]
InP	15.5	none	Au	direct deposition	[25]

2. Hybrid mirror development for InGaSb-VECSEL

The hybrid mirror fabrication for the GaSb-based VECSEL is based on working procedures specially adapted to the GaSb material system and described in more detail in this paper. Initially, we were motivated to work with a gold metal mirror because of its superior reflectivity. However unexpected problems described here led us to choose a copper metal mirror which provided superior cw VECSEL performance with only 10.5 instead of 19.5 DBR layer pairs for an operation wavelength at 2 µm.

With regards to a gold metal mirror approach, we faced the following problems. A direct deposition approach was initially considered, where a gold layer was deposited on the backside of the highly reflective DBR. This approach was not successful due to the poor adhesion of gold to the semiconductor. This can be overcome by removing native oxides from the semiconductor surface with an argon plasma etching process before metal evaporation. We faced, however, another unexpected problem while indium-soldering the VECSEL chip to its heat-sink. The gold mirror diffused into the semiconductor during the vacuum soldering process which is performed just above the indium melting temperature of 156 °C. To stop diffusion, a 20-nm thin dielectric material as a diffusion barrier layer was grown on the chip before evaporating the gold metal layer. Different dielectric diffusion barriers were tested using various deposition techniques. Fused silica grown at 300 °C with PECVD has shown reliable results with consistent growth rates and sufficiently dense coatings. However, in the end, the adhesion of gold to the fused silica was too low to withstand the mechanical stress during substrate removal. Metallic diffusion barriers were not considered even though they have superior thermal properties compared to dielectrics, but they introduce significantly higher losses which is detrimental for this application.

We therefore started to investigate alternative metal mirrors. Aluminium and copper were considered because they have both a high intrinsic reflectance at 2 µm and a limited diffusion through SiO_2. Silver was not available for us and could potentially be an option for future research studies. To check the adhesion, thin metal films of 100 nm were evaporated onto bare GaSb with a SiO_2 diffusion barrier. All metals are deposited using electron beam evaporation. To assess the adhesion, we performed a scratch and a tape test. For the scratch test, the metal surface is scratched with a sharp device. If the metal peels off the sample, the scratch test is considered failed. For the tape test, we used Scotch tape attached to the sample and then peeled it off. If the metal peels off with the Scotch tape, the tape test is considered failed. Aluminium passed both tests whereas copper passed the scratch test but failed the tape test and in comparison, gold failed both tests. Nevertheless, copper was chosen as a mirror material due to its slightly higher reflectivity compared to aluminium, allowing for a DBR with fewer mirror pairs. Combining 10.5 $AlAs_{0.08}Sb_{0.92}$/GaSb DBR layer pairs with a copper mirror and a 20-nm SiO_2 thin diffusion barrier we obtain the desired >99.9% reflectivity from the hybrid mirror. Copper withstood the mechanical stress during the processing and showed no degradation after many temperature cycles (from $-10\,^{\circ}$C to $20\,^{\circ}$C) during the laser testing. Therefore, copper was considered to be suitable for VECSEL integration within our academic research effort (Fig. 1).

2.1. InGaSb VECSEL gain chip design

The semiconductor structure of our 2-µm VECSEL chip (Fig. 1) was grown with molecular beam epitaxy (MBE) in the FIRST cleanroom facility at ETH Zürich (see more information in the methods section). The structure is grown in reverse growth order for flip-chip processing and backside-cooling. Figure 1(a) shows the vertical layer design with regards to the refractive index of the different materials inside the semiconductor VECSEL chip overlapped with a cross-section scanning electron microscope (SEM) image of the structure. The semiconductor VECSEL chip consists of 5 x 3 $In_{0.27}Ga_{0.73}Sb$/GaSb QWs for the gain and a 10.5-pair $AlAs_{0.08}Sb_{0.92}$/GaSb DBR. The VECSEL chip is finished on the highly reflective side with a copper layer to form a hybrid metal-semiconductor mirror (not shown here) and on the other side with a standard PECVD grown $\lambda/4$-thick Si_3N_4 anti-reflection (AR) coating for the transition into free space inside the linear standing-wave laser cavity.

Fig. 1(b) shows an XRD measurement of the as-grown structure, confirming monolithic growth and good interface quality as seen in the clear interference fringes from the structure. This is also confirmed with the cross-section SEM image in Fig. 1(a). The side peaks in the XRD measurement at lower angles arise from the fact that the ternary QWs are compressively strained compared to the GaSb substrate.

In Fig. 1(c), the spectral reflectance of the final hybrid-mirror VECSEL chip is shown together with a photoluminescence (PL) measurement. The absorption dip in the stopband matches the PL wavelength which lies on the blue edge of the stopband. This is intentional in the design since the emission will redshift during operation taking into account the heating of the active region (i.e. assumed to be 50 °C). The integration of the copper metal mirror into the VECSEL chip design introduces a destructive interference between the metal mirror and the DBR which causes a reduction in reflectance on the red edge of the DBR stopband (Fig. 1(c), red and orange lines). This reflectance dip is shifted by adding an $AlAs_{0.08}Sb_{0.92}$ phase-matching layer between metal and semiconductor in the design of the structure. The phase dip is also observed to decline with an increasing number of DBR layer pairs. The measured reflectance (red line) is slightly redshifted compared to the design (dashed orange line) because of small growth variations. The processed VECSEL chip shows more losses outside the stopband than predicted by the simulation. We attribute these losses to imperfections on the interfaces between semiconductor, dielectric, and metal mirror which leads to scattering.

As shown in Fig. 1(d) the active region with the 5 x 3 $In_{0.27}Ga_{0.73}Sb$/GaSb QWs are placed around the antinodes of the intensity standing wave pattern which corresponds to a more resonant periodic gain arrangement. The QW thickness is 8 nm and the GaSb barrier thickness is 10 nm. In between the QWs a lattice-matched 10-nm thick $AlAs_{0.08}Sb_{0.92}$ is used to ensure carrier confinement. Carriers in the GaSb barrier layers around the $In_{0.27}Ga_{0.73}Sb$ wells are exited by the

Optical Materials EXPRESS

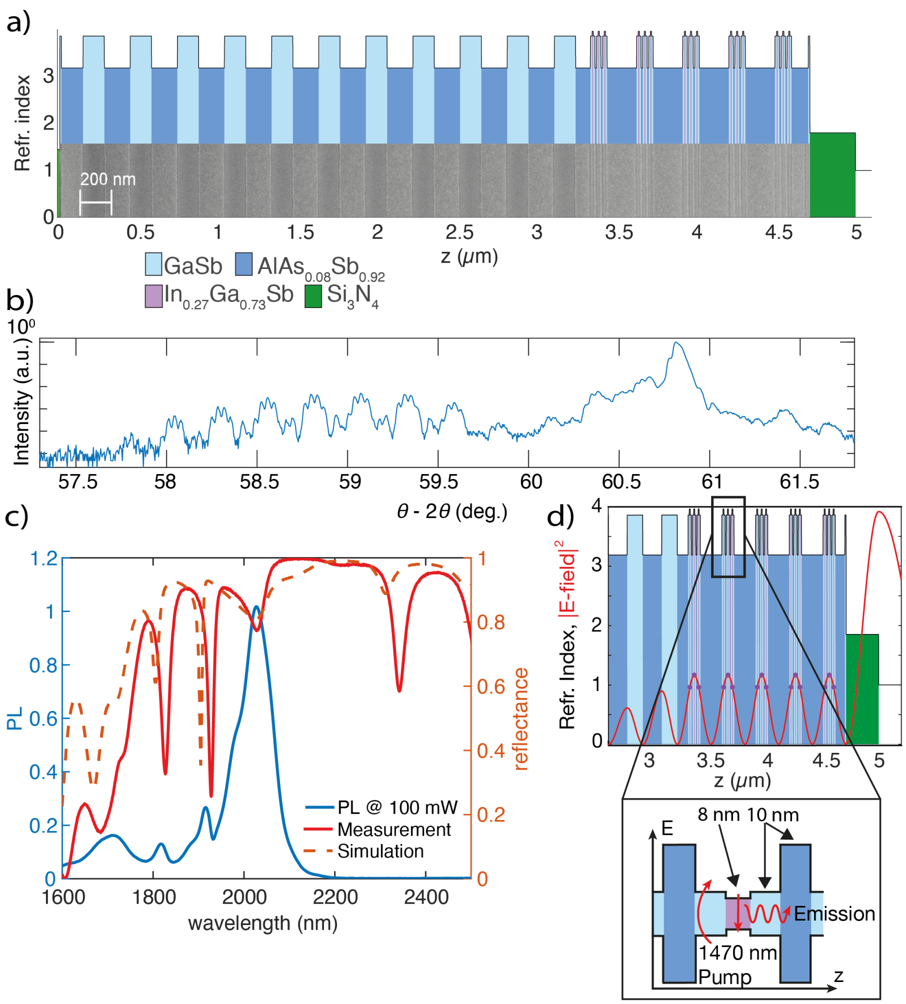

Fig. 1. 2-μm VECSEL gain chip design and standard characterization. a) Cross-section scanning electron microscopy (SEM) image overlapped with gain mirror design. The structure consists of 5 x 3 $In_{0.27}Ga_{0.73}Sb$ gain quantum wells (QWs) placed on top of an $AlAs_{0.08}Sb_{0.92}$/GaSb DBR with 10.5 layer pairs. b) X-ray diffraction (XRD) measurement of the as-grown semiconductor structure. c) Spectral reflectance measurement (red) and simulation (orange dashed). Photoluminescence (PL) measurement (blue). d) Resonant periodic gain QW arrangement in the active region. Zoom in: Bandgap energy as function of distance z along the laser cavity mode direction of a single QW. The 8-nm thin $In_{0.27}Ga_{0.73}Sb$ QW is sandwiched between two 10-nm thin GaSb barrier layers for barrier pumping with a commercial Dilas 1470-nm pump diode array with an M^2 of 94. The carriers in the QW are confined on both sides by a 10-nm thin $AlAs_{0.08}Sb_{0.92}$ layer.

Optical Materials EXPRESS

1470-nm pump light and are confined in the QW by the $AlAs_{0.08}Sb_{0.92}$ layers to stop diffusion out of the QWs. The Si_3N_4 AR coating increases the field intensity in the active region and thus the gain. The gain mirror structure is designed for antiresonance with a field intensity enhancement of 1.2 [26] to allow for wide bandwidth suitable for modelocking in the future.

3. Results and discussion

3.1. VECSEL cavity design and thermal resistance measurement

The optically pumped linear standing-wave VECSEL cavity is shown in Fig. 2(a). The VECSEL chip is pumped with a commercial fiber-coupled multimode 1470-nm diode laser bar with an M^2 of 94, with the pump beam at 45° angle of incidence and focussed down to a circular pump spot of $\sim 350\,\mu$m diameter using a combination of circular and cylindrical lenses. The 2 % output coupler with a radius of curvature -100 mm allows us to match the laser mode size with the pump spot size for a cavity length of 7.5 cm. The chip is temperature stabilized by a Peltier-element. The inset in Fig. 2(a) shows the laser spectrum of the VECSEL recorded for a fixed pump power and heat-sink temperature. We find the center wavelength by fitting a Gaussian in each recorded optical spectrum. See more info on commercial devices and laser performance characterization in the methods section. The setup allows for automated measurement of output power, reflected pump power, beam profile and emission spectrum as a function of pump power and Peltier-cooled heat-sink temperature. The center lasing wavelength is measured as a function of heat-sink temperature and pump power as shown in Fig. 2(b). We then can extract the thermal resistance by determining the wavelength shift for constant heat-sink temperatures with increasing pump powers and vice versa. By averaging the slopes, we can then calculate the thermal resistance according to [27]

$$R_{th} = \frac{\Delta\lambda}{\Delta P_{pump}} \left(\frac{\Delta\lambda}{\Delta T}\right)^{-1} . \tag{1}$$

Theoretical estimates for the thermal resistance of a similar system were done by [24].

3.2. VECSEL gain chip performance comparison

Here we compare the cw lasing performance and thermal resistance of three in-house fabricated optically pumped InGaSb VECSEL chips in a linear standing-wave laser cavity as shown in Fig. 1 and Fig. 2. Figure 3 shows the recorded powerslopes (i.e. output power as a function of incident pump power) with the beam profile at an output power of 1 W for (a) and (b) and just above the laser threshold for (c) (from previous work, see [14]) and the final VECSEL chip thickness. The VECSEL chips are bonded to a diamond heat spreader and mounted on a Peltier-stabilized copper heat-sink as shown in Fig. 2(a). The powerslopes are taken for heat-sink temperatures ranging from −10 °C to 10 °C (see color code in Fig. 3). Maximum output power of up to 3 W can be reached with the hybrid-mirror VECSEL (Fig. 3(a)) with pump powers of up to 20 W before the thermal rollover occurs. The inset beam profiles in Fig. 3 indicate gaussian beam shapes and single-mode operation with good beam quality. All three devices show the typical decrease in lasing efficiency of semiconductor lasers at higher pump powers.

The reflected pump of all three devices was between 3 to 5 %. This can be explained by the fact that the DBR in the VECSEL is not designed for the pump wavelength and thus a significant portion of the pump light is absorbed in places not contributing to lasing such as the GaSb layers in the DBR (see Fig. 1(d)). There was no significant difference in reflected pump power for the thin structures compared to the thicker 19.5-pair DBR VECSEL chip. Theoretically, ≈34 % of the pump power is absorbed in the QW layers with one single pass. Future VECSEL chips can incorporate an additional pump DBR before the lasing DBR to increase pump efficiency and no additional pump absorption in the lasing DBR. For each point in the powerslope measurements, the full laser spectrum is recorded. From the data, the thermal resistance for all three devices

Optical Materials EXPRESS

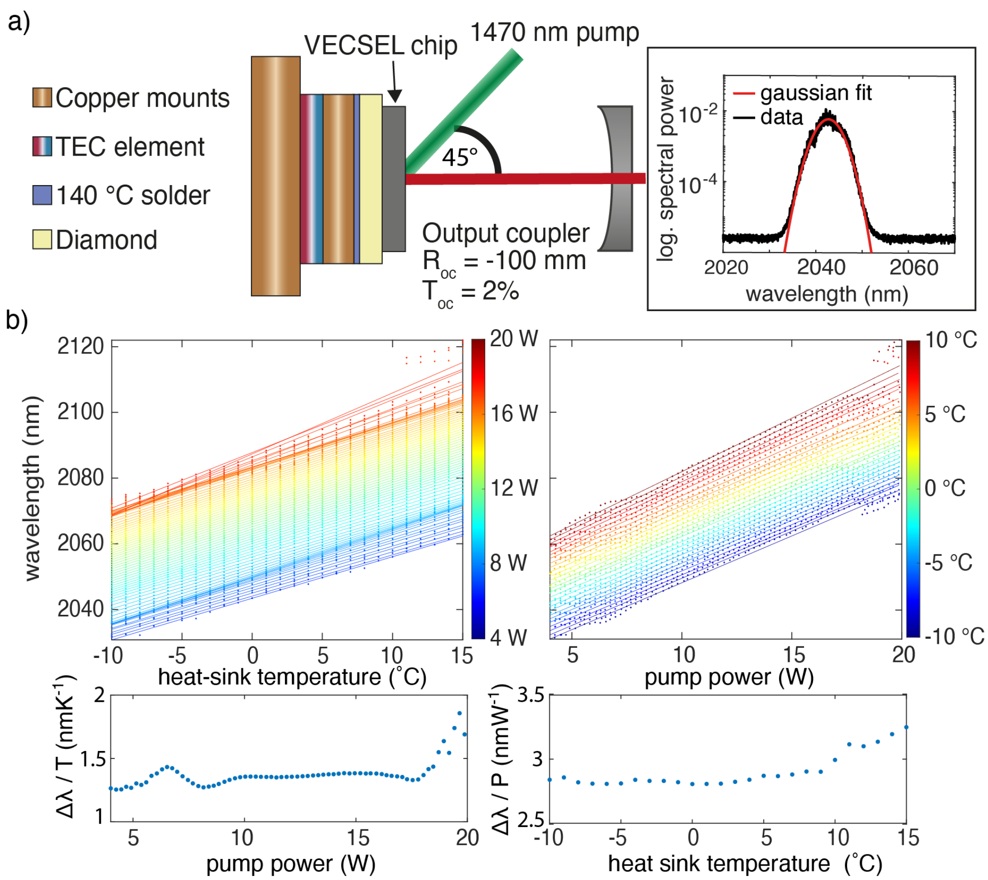

Fig. 2. a) Straight VECSEL cavity. b) Example thermal resistance measurement. Wavelength shift is determined for constant pump powers and constant heat-sink temperatures.

is calculated according to Eq. (1). The hybrid mirror InGaSb VECSEL using copper and 10.5 DBR pairs has a thermal resistance of $(2.12\pm0.19)\,\mathrm{K\,W^{-1}}$. To date, this is the lowest thermal resistance reported for flip-chip-processed InGaSb-based VECSEL gain chips. It is a significant decrease in thermal resistance compared to the non-hybrid VECSEL using 19.5 DBR layer pairs which has a thermal resistance of $(2.79\pm0.16)\,\mathrm{K\,W^{-1}}$. The lasing threshold without the copper mirror (Fig. 3(b)) is significantly higher and the measured spectral reflectance outside the stopband is lower than in the simulations. Also, the measured spectral reflectance outside the stopband is lower than in the simulations. Without the copper mirror the 10.5-pairs DBR results in a simulated reflectivity of only 95.2 %. Additional losses in the hybrid-mirror design (as shown in Fig. 1(a)) can arise from scattering on imperfections on the interfaces between metal, dielectric and semiconductor. In addition, we expect very few losses from the SiO_2 layer due to its transmission at 2 µm. Improvement of the interface and processing quality is expected to lower the lasing threshold close to the value of the 19.5-pairs DBR with a theoretical reflectivity of 99.9 %. The details of all structures that are compared are summarized in Table 2.

Optical Materials EXPRESS

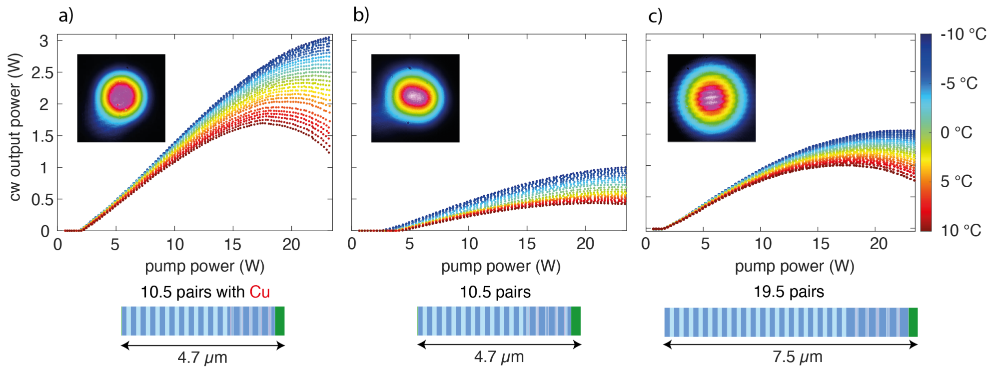

Fig. 3. Powerslope measurements for the three 2-µm InGaSb VECSEL. a) Hybrid-mirror VECSEL design using 10.5 DBR layer pairs plus copper mirror. b) VECSEL design using 10.5 DBR layer pairs without copper. c) VECSEL design using 19.5 DBR pairs.

Table 2. Summary of the three InGaSb VECSEL performances with the same active region. The hybrid-mirror VECSEL uses 10.5 DBR pairs designed to be combined with a copper metal mirror and has a theoretical reflectivity of >99.9 % whereas without the copper mirror it has a theoretical reflectivity of 95.2 %. The full semiconductor-based VECSEL contains a 19.5-pairs DBR and has a theoretical reflectivity of 99.9 %. In all cases a 2 % output coupler was used for a lasing wavelength around 2 µm [14,15]

VECSEL gain chip	10.5 layer pairs + Cu	10.5 layer pairs	19.5 layer pairs
mirror pairs	10.5	10.5	19.5
simulated relfectivity	>99.9 %	95.2 %	99.9 %
semiconductor thickness	4.7 µm	4.7 µm	7.5 µm
thermal resistance	$(2.12\pm0.19)\,\mathrm{K\,W^{-1}}$	$(2.36\pm1.20)\,\mathrm{K\,W^{-1}}$	$(2.79\pm0.16)\,\mathrm{K\,W^{-1}}$
lasing threshold	2.32 W	2.93 W	1.91 W
max. cw output power	3.05 W	1.01 W	1.55 W

4. Conclusion and outlook

We present the first backside-cooled, InGaSb-based VECSEL using a hybrid metal-semiconductor Bragg reflector. The fabrication procedure was developed for a lasing wavelength of around 2 µm and compared to a VECSEL with a semiconductor-based DBR. The technology allowed us to reduce the thickness of the VECSEL chip from 7.5 µm to 4.7 µm resulting in a thermal resistance reduction from $(2.79\pm0.16)\,\mathrm{K\,W^{-1}}$ to $(2.12\pm0.19)\,\mathrm{K\,W^{-1}}$. Record high average cw output power of 3 W was achieved for the backside-cooled hybrid-mirror InGaSb VECSEL. This is more than three times the previous record output power for backside-cooled InGaSb VECSELs using only a semiconductor DBR [14].

The fabrication challenges of adhesion and diffusion were overcome by the choice of copper for the metal mirror and by using a thin 20-nm layer of PECVD-grown fused silica. Replacing the classic mirror materials of aluminium and gold with copper is a compromise between mechanical interface stability and spectral reflectance of the metal at 2 µm. Improvement in the lasing threshold could possibly be achieved by increasing the interface quality between metal, dielectric and semiconductor to reduce scattering losses which are in the sub-percent range.

This hybrid-mirror technology will become even more important for better pump efficiency and VECSELs at longer wavelengths with even thicker DBR layer pairs. The diffusion barrier will need to be adapted due to the strong absorption features of SiO_2 between 2.5 and 3 µm wavelength range. Promising alternatives to be investigated are Al_2O_3 and TiO_2.

Optical Materials EXPRESS

Further efforts towards higher output power of backside-cooled SWIR VECSELs will require the integration of an additional pump-reflecting DBR in the design to reduce the amount of absorbed pump power in the laser DBR. Adding such a mirror increases the overall VECSEL chip thickness but reduces the overall heat load and increases the optical-to-optical efficiency. The integration of the pump DBR is also an important step towards the fully integrated modelocked MIXSEL [28] and dual-comb modelocking [4]. These are important milestones for the many applications in the 2 to 3-µm wavelength range discussed in the introduction.

5. Methods

5.1. Growth and processing

The semiconductor structure is grown in a VEECO GEN III MBE reactor. The growth temperatures for the active region, the DBR and the etch stop are 480 °C. The growth temperature is controlled with two thermocouples and verified with a black body radiation measurement using a kSA BandiT. For the Sb, a cracker with a cracking zone at 900 °C is used. Careful adjustment of the As/Sb ratio ensures the lattice matching for the ternary materials $AlAs_{0.08}Sb_{0.92}$ and $InAs_{0.92}Sb_{0.08}$ (etch stop). To reach the required low Sb flux in the etch stop, the Sb bulk temperature is 511 °C and is increased to 533 °C for the rest. The substrate is a Te-doped 2 ″ (001)-GaSb wafer of 500 µm thickness. Growth is performed in reverse order and it is started with the $InAs_{0.92}Sb_{0.08}$ etch-stop layer, followed by the active region and ended with the DBR. The wafer is cleaved into 4.5 x 4.5 mm pieces which are then individually cleaned with acetone and isopropyl alcohol in an ultrasonic bath. The samples are then coated with 20-nm thick PECVD grown SiO_2 using an Oxford Instruments PECVD Plasma Pro 80 at a growth temperature of 300 °C. Next, the samples are coated with 100-nm thick layer of copper for the hybrid mirror and 10-nm thick layer of platinum to prevent oxidation of the copper. The platinum also stops the later added soldering metals from diffusing into the mirror. All the subsequent processing steps are described in detail in the methods section of [14].

5.2. Device characterization

XRD measurements are performed with a Seifert XRD 3003 PTS-HR. Samples for SEM imaging are freshly cleaved and mounted to ensure a clean interface. SEM pictures are taken with a Zeiss Ultra 55 plus using the in-lens detector and an accelerator voltage of 5 keV. Photoluminescence and linear reflectance measurements are performed with a Bruker VERTEX 80v FT-IR using a liquid nitrogen-cooled InSb detector and a globar light source is used for the linear reflectance measurement. The PL unit is attached to the FT-IR and uses a 1064 nm excitation laser. For the thermal characterization measurements, a 1470-nm DILAS pump diode bar is used reaching up to 40 W multimode cw power with an M^2 of 94. Beam profiles are recorded using a DataRay WinCamD-IR-BB. The optical spectra are recorded with a Yokogawa AQ6376 OSA using 1-nm resolution.

Funding. European Research Council (ERC advanced grant 787097 ONE-MIX).

Acknowledgments. We thank the FIRST clean room facility at ETH Zürich.

Disclosures. The authors declare no conflicts of interest.

Data availability. Data underlying the results presented in this paper are not publicly available at this time but may be obtained from the authors upon reasonable request.

References

1. M. Kuznetsov, F. Hakimi, R. Sprague, and A. Mooradian, "High-power (> 0.5-w cw) diode-pumped vertical-external-cavity surface-emitting semiconductor lasers with circular TEM_{00}beams," IEEE Photonics Technol. Lett. **9**(8), 1063–1065 (1997).
2. U. Keller and A. C. Tropper, "Passively modelocked surface-emitting semiconductor lasers," Phys. Rep. **429**(2), 67–120 (2006).

Optical Materials EXPRESS

3. B. W. Tilma, M. Mangold, C. A. Zaugg, S. M. Link, D. Waldburger, A. Klenner, A. S. Mayer, E. Gini, M. Golling, and U. Keller, "Recent advances in ultrafast semiconductor disk lasers," Light: Sci. Appl. **4**(7), e310 (2015).
4. S. M. Link, A. Klenner, M. Mangold, C. A. Zaugg, M. Golling, B. W. Tilma, and U. Keller, "Dual-comb modelocked laser," Opt. Express **23**(5), 5521–5531 (2015).
5. J. Pupeikis, B. Willenberg, S. L. Camenzind, A. Benayad, P. Camy, C. R. Phillips, and U. Keller, "Spatially multiplexed single-cavity dual-comb laser," Optica **9**(7), 713 (2022).
6. C. R. Phillips, B. Willenberg, A. Nussbaum-Lapping, F. Callegari, S. L. Camenzind, J. Pupeikis, and U. Keller, "Coherently averaged dual-comb spectroscopy with a low-noise and high-power free-running gigahertz dual-comb laser," arXiv, arXiv:2211.01368 (2022).
7. S. M. Link, D. J. H. C. Maas, D. Waldburger, and U. Keller, "Dual-comb spectroscopy of water vapor with a free-running semiconductor disk laser," Science **356**(6343), 1164–1168 (2017).
8. J. Nürnberg, C. G. E. Alfieri, Z. Chen, D. Waldburger, N. Picqué, and U. Keller, "An unstabilized femtosecond semiconductor laser for dual-comb spectroscopy of acetylene," Opt. Express **27**(3), 3190 (2019).
9. B. Willenberg, C. R. Phillips, J. Pupeikis, L. Liebermeister, R. Kohlhaas, B. Globisch, and U. Keller, "Rapid THz-TDS enabled by single-cavity dual-comb gigahertz laser," EPJ Web Conf. **267**, 01038 (2022).
10. J. Pupeikis, B. Willenberg, F. Bruno, M. Hettich, A. Nussbaum-Lapping, M. Golling, C. P. Bauer, S. L. Camenzind, A. Benayad, P. Camy, B. Audoin, C. R. Phillips, and U. Keller, "Picosecond ultrasonics with a free-running dual-comb laser," Opt. Express **29**(22), 35735–35754 (2021).
11. J. Pupeikis, W. Hu, B. Willenberg, M. Mehendale, G. Antonelli, C. Phillips, and U. Keller, "Efficient pump-probe sampling with a single-cavity dual-comb laser: Application in ultrafast photoacoustics," Photoacoustics **29**, 100439 (2023).
12. R. Liao, H. Tian, W. Liu, R. Li, Y. Song, and M. Hu, "Dual-comb generation from a single laser source: Principles and spectroscopic applications towards mid-IR - a review," J. Phys. Photonics **2**(4), 042006 (2020).
13. P. Holl, M. Rattunde, S. Adler, A. Bächle, E. Diwo-Emmer, R. Aidam, and J. Wagner, "Gasb-based 2.0 µm sdl with 17 W output power at 20 °C," Electron. Lett. **52**(21), 1794–1795 (2016).
14. M. Gaulke, J. Heidrich, B. O. Alaydin, M. Golling, A. Barh, and U. Keller, "High average output power from a backside-cooled 2-µm InGaSb VECSEL with full gain characterization," Opt. Express **29**(24), 40360 (2021).
15. J. Heidrich, M. Gaulke, M. Golling, B. O. Alaydin, A. Barh, and U. Keller, "324-fs pulses from a sesam modelocked backside-cooled 2-µm vecsel," IEEE Photonics Technol. Lett. **34**(6), 337–340 (2022).
16. M. Y. A. Raja, S. R. Brueck, M. Osinski, C. F. Schaus, J. G. McInerney, T. Brennan, and B. Hammons, "Resonant periodic gain surface-emitting semiconductor lasers," IEEE J. Quantum Electron. **25**(6), 1500–1512 (1989).
17. M. Guina, A. Rantamki, and A. Härkönen, "Optically pumped VECSELs: review of technology and progress," J. Phys. D: Appl. Phys. **50**(38), 383001 (2017).
18. S. Koizumi, C. Nebel, and M. Nesladek, *Physics and Applications of CVD Diamond* (John Wiley & Sons, 2008).
19. Q. Zheng, C. Li, A. Rai, J. H. Leach, D. A. Broido, and D. G. Cahill, "Thermal conductivity of GaN, ^{71}GaN, and SiC from 150 k to 850 k," Phys. Rev. Materials **3**(1), 014601 (2019).
20. J. Carvill, *Mechanical Engineer's Data Handbook* (Butterworth-Heinemann, 2014).
21. A. Rantamaki, E. J. Saarinen, J. Lyytikainen, J. Heikkinen, J. M. Kontio, K. Lahtonen, M. Valden, and O. G. Okhotnikov, "Thermal management in long-wavelength flip-chip semiconductor disk lasers," IEEE J. Sel. Top. Quantum Electron. **21**(6), 336–342 (2015).
22. E. J. Saarinen, K. Lahtonen, M. Valden, and O. G. Okhotnikov, "High power semiconductor disk laser with a semiconductor-dielectric-metal compound mirror," Appl. Phys. Lett. **104**(10), 101110 (2014).
23. K. Gbele, A. Laurain, J. Hader, W. Stolz, and J. V. Moloney, "Design and fabrication of hybrid metal semiconductor mirror for high-power VECSEL," IEEE Photonics Technol. Lett. **28**(7), 732–735 (2016).
24. M. Devautour, A. Michon, G. Beaudoin, I. Sagnes, L. Cerutti, and A. Garnache, "Thermal management for high-power single-frequency tunable diode-pumped VECSEL emitting in the near- and mid-IR," IEEE J. Sel. Top. Quantum Electron. **19**(4), 1701108 (2013).
25. J. P. Tourrenc, S. Bouchoule, A. Khadour, J. C. Harmand, A. Miard, J. Decobert, N. Lagay, X. Lafosse, I. Sagnes, L. Leroy, and J. L. Oudar, "Thermal optimization of 1.55 µm OP-VECSEL with hybrid metal-metamorphic mirror for single-mode high power operation," Opt. Quantum Electron. **40**(2-4), 155–165 (2008).
26. G. J. Spühler, K. J. Weingarten, R. Grange, L. Krainer, M. Haiml, V. Liverini, M. Golling, S. Schn, and U. Keller, "Semiconductor saturable absorber mirror structures with low saturation fluence," Appl. Phys. B: Lasers Opt. **81**(1), 27–32 (2005).
27. J. P. Perez, A. Laurain, L. Cerutti, I. Sagnes, and A. Garnache, "Technologies for thermal management of mid-IR Sb-based surface emitting lasers," Semicond. Sci. Technol. **25**(4), 045021 (2010).
28. D. J. Maas, A. R. Bellancourt, B. Rudin, M. Golling, H. J. Unold, T. Südmeyer, and U. Keller, "Vertical integration of ultrafast semiconductor lasers," Appl. Phys. B: Lasers Opt. **88**(4), 493–497 (2007).